

# On the Interfacial Properties of Carbon Nanotube Based Composites

Roham Rafiee<sup>\*1</sup>, Mohammad Mahdavi<sup>2</sup>

<sup>1,2</sup>Composites Research Laboratory, Faculty of New Sciences and Technologies,  
University of Tehran, Tehran 1439955941, Iran

<sup>\*1</sup>Roham.Rafiee@ut.ac.ir

### I. INTRODUCTION

The extraordinary properties of Carbon Nanotubes (CNTs) have stimulated researchers to use them as the reinforcing agent in polymeric composites and thus nano-composites a new generation of materials has been born [1]. The efficiency of CNT in reinforcing polymer is defined by different factors at different scale. The key factor at micro/nano scale is the load transferring issue from resin to CNT and other parameters like agglomeration, waviness and inhomogeneous dispersion of CNTs are captured at meso and/or macro scales [2-8]. At the level of micro, the interaction between CNT and surrounding polymer has to be studied through simulating the interphase region. The interphase region accounts for load transferring from the matrix to the CNT which naturally takes places through weakly non-bonded van der Waals (vdW) interactions. Improving load transferring mechanism, chemical functionalization of CNT provides transversely powerful covalent bond between CNT and polymer. This procedure will cause defects in the nanostructure of CNT which will be led to a reduction in CNT Young's modulus [7, 9-15]. Moreover, vacancy defects maybe also induced into the CNT during its growth process.

Due to the experimental challenges at nano-scale, theoretical modeling has been extensively employed by researchers to predict the mechanical performance of CNT reinforced polymers. Mechanical behavior of nanocomposites at nano/micro scales can be simulated using atomistic modelling techniques. Molecular Dynamic (MD), Monte Carlo (MC) and Ab Initio methods are the main categories of atomistic modelling. In MD and MC approaches, the positions of atoms are described employing second Newton's law. Schrödinger wave equation is solved in Ab initio method on the basis of quantum mechanics approach. Further to that, Density Functional Theory (DFT) and Tight Bonding Molecular Dynamic (TBDM) are other recently established atomistic modelling methods [7]. Several attempts have been done to estimate the Young's Modulus of CNT-based composites using different atomistic techniques. MD Tersoff-Brenner (TB) potential [16-23], MD-REBO [9, 24-26], MD-COMPASS [27, 28], DFT [15, 22, 29, 30], TBDM [31-35] and Ab initio [17, 34-37] have been employed by different researchers in literature.

It should however be pointed out that DFT, TBDM and Ab initio methods are in need of considerable runtime for each simulated system. This is arisen from solving Schrödinger equations for each atom based on quantum mechanics. MD simulations are preferred whereas acceptable level of accuracy can be achieved using less complex formulation with less required run time. Thus, MD method is chosen to be the subject matter of study within this chapter.

With this idea in mind, this chapter aims to study the influence of chemical functionalization on the Young's modulus of the representative volume element consisting of CNT and surrounding polymer at nano-scale using MD simulation. The remaining sections of the chapter are constructed as below.

Firstly, Young's modulus of isolated CNT is obtained. The Young's moduli of non-defected CNTs are predicted using two different non-linear force fields. Then, the influence of CNTs morphology on the results is comprehensively analyzed.

Secondly, the reduction level in the Young's modulus of defected CNT is quantified assuming numbers and locations of defects as random parameters. Therefore, stochastic MD simulations are properly conducted capturing aforementioned randomness. The Young's moduli of non-defected and defected CNTs are compared and the influence of vacancy defects on the CNT Young's modulus is discussed.

Finally, theoretical characterization of the interaction between CNT and surrounding polymer is presented using MD simulation. Embedded CNT in polymer is simulated with a particular concentration on the interaction between CNT and polymer. The influence of chemical functionalization on elastic properties of nanocomposites is discussed at micro level. Stochastic analysis is conducted with treating numbers of established cross links between CNT and polymer and their positions as random parameters.

## II. MODELING ISOLATED CNT

Utilizing atomistic modelling and/or continuum modelling approaches, numerous researchers have predicted Young's Modulus of isolated and/or non-defected CNTs. The conducted investigations have been critically reviewed by Shokrieh and Rafiee [38]. As the widely accepted value, the Young's Modulus of non-defected CNT is estimated about 1 TPa. However, literature shows that limited efforts have been devoted to estimate the influence of defects on the Young's Modulus of CNTs.

In this perspective, mechanical properties of defected CNTs have been analyzed employing MD simulations. For instance, Yuan and Liew [15] simulated (5, 5) and (10, 10) defected CNTs at high temperature above 2000 K and reported that for 2% induced vacancy defect, about 17% reduction in Young's Modulus of CNT was observed. Analyzing the influence of vacancy defects in different temperature, three types of CNTs have been simulated by Jeng et al. applying TB potential [12]. For the case of a CNT with chiral index of (10, 0), the Young's Modulus have been found to be reduced 2.7%. The influence of temperature on the results has been also reported by them implying on reduction in mechanical properties of CNT with increasing temperature [12]. Applying COMPASS force field, Sharma et al. have deterministically simulated defected CNT with chiral index of (9, 9) in presence of one and four vacancy defects [14]. In another research, Sharma et al. [28] have studied the effect of inducing one to four defects into (4, 4) CNT nanostructure. The obtained results showed that the Young's Modulus of the defected CNTs decrease 6% to 17% for one to four vacancy defects. Fefey et al. [39] evaluated the influence of two vacancy defects on (6, 6) CNT using linear potentials. Placing defect at radial and longitudinal directions, 8% and 4% reduction in Young's Modulus have been identified, respectively. Comparing TB potentials and TBDM method, Talukdar and Mitra [23] have simulated (5, 0) CNT accommodating one and two defects. It was reported that regardless of number of induced defects, the level of reduction in Young's Modulus of defected CNT for the case of TBDM method is higher than that of TB potential [25].

Concentrating on MD simulations, it has shown in literature that deterministic simulations are conducted on defected CNT and deterministic numbers and positions of defects have been studied. Moreover, the influence of CNT morphology has not been studied. In this section, the influence of vacancy defect on the Young's modulus of CNT is investigated using stochastic MD simulation. Performing full stochastic simulations, numbers of induced defects and its corresponding location along the circumferential and axial direction of CNT are taken into account as random variables. The simulations are conducted employing non-linear interatomic potentials to examine how they are affecting the results. Performing a parametric study, the important role of CNT diameter and chirality on the results has been characterized.

### A. Modeling Fundamentals

The concept of MD simulations and involved parameters are briefly explained in this section.

A combination of individual Potential Energy Functions (PEFs) is called a force-field function and used to describe the total interactions in a molecular system. Each individual PEF is responsible to address a certain aspect of the entire interactions. Bond stretching, bond-angle bending, improper dihedral-angle bending, inversion-angle bending and non-bonded vdW and electrostatic interactions are constitutive terms of the force-field. For a model with a united atom such as Single Walled CNT (SWCNT), vdW and electrostatic interactions are neglected. The first term of a force-field (i.e. bond stretching) is the most dominant one compared to the remaining terms [40]. Bond stretching and bond bending terms are considered for the purpose of more accurate modeling.

There are three main PEFs for modeling CNT such as AMBER [41], Tersoff-Brenner first-generation (TB) [42] and the Brenner second-generation (REBO) [43]. Linear terms are employed in AMBER PEF for modeling interatomic interactions and non-linear terms are used to construct TB and REBO PEFs. Both aforementioned non-linear potentials are used in this research for the purpose of comparative study.

Two-body PEFs describing bonded interactions within CNTs have also been proposed. Two-body potential consists of two components, bond-stretching and bond-bending parts.

The bond stretching term of the Brenner first-generation potential is modelled in the form of pair-wise interactions using Morse-type functions. The first generation of Tersoff potentials are given by the following equation [42]:

$$V^{TB}(r_{ij}) = f_c(r_{ij})[V^R(r_{ij}) + b_{ij}V^A(r_{ij})] \quad (1)$$

where, the function  $V^R(r_{ij})$  represents the repulsive pair-wise interaction, for example the core-core interaction, and the function  $V^A(r_{ij})$  represents the attractive potential due to valence electrons.

$$V^R(r_{ij}) = \frac{D_{ij}}{S_{ij} - 1} e^{-\sqrt{2S_{ij}}\beta_{ij}(r_{ij}-r_0)} \quad (2)$$

$$V^A(r_{ij}) = -\frac{D_{ij}S_{ij}}{S_{ij}-1} e^{-\sqrt{\frac{2}{S_{ij}}}\beta_{ij}(r_{ij}-r_0)} \quad (3)$$

where  $D_{ij}=9.648 \times 10^{-19}$  N.m,  $S_{ij}=1.22$ ,  $r_0=1.4507$  Å and  $\beta_{ij}=2.625 \times 10^{10}$  m<sup>-1</sup> [44].

Decreasing the distance between the atoms, finite values are reported by both potential terms in the Morse-type form and thus the option of modeling the energetics of atomic collision processes is limited [40]. Moreover, it was found that the Morse-type function was too restrictive to simultaneously fit the equilibrium distances, energies and force constants for carbon-carbon bonds [40]. More accurate analytical functions and an expanded fitting database are employed to construct the second-generation Brenner potential intermolecular interactions. These improvements offer significantly more refined description not only for the bond lengths, energies and force constants of hydrocarbon molecules, but also for the elastic properties, interstitial defect energies and surface energies.

The REBO potential functions are expressed as:

$$V^{REBO}(r_{ij}) = f_c(r_{ij})[V^R(r_{ij}) + b_{ij} V^A(r_{ij})] \quad (4)$$

$$V^R(r_{ij}) = f_c(r_{ij})[1 + \frac{Q_{ij}}{r_{ij}}]A_{ij}e^{-\alpha_{ij}r_{ij}} \quad (5)$$

$$V^A(r_{ij}) = -f_c(r_{ij}) \sum_{n=1,3} B_{ijn} e^{-\beta_{ijn}r_{ij}} \quad (6)$$

where  $f_c$  is cut off functions in both potentials that are available in references [42, 43]. The associated parameters with the REBO potential pertinent to the carbon-carbon interaction are presented in Table 1.

TABLE 1 PARAMETERS OF THE REBO POTENTIALS FOR CARBON-CARBON INTERACTIONS [40]

B1 (eV)	B2 (eV)	B3 (eV)	$\alpha$ (Å <sup>-1</sup> )	$\beta_1$	$\beta_2$	$\beta_3$	Q	A
12388.79	17.567	30.714	4.746	4.720	1.433	1.382	0.313	10953.544

Moreover, bond-bending term is expressed by [40]:

$$H(\cos(\theta)) = E(\cos(\theta) - \cos(\theta_0))^2 \quad (7)$$

where  $E = 67.1383$  kcal/mol, and  $\cos\theta_0 = -0.5$  for C-C bonds [40].

LAMMPS software is utilized for performing aforementioned modelling procedure [45].

### B. Modeling Non-defected CNT

Following the explained procedure in previous section, different CNTs with various chiral indices and diameters constructed. One end of CNT is restricted from any movement and the other end is subjected to a constant velocity is applied to the other end. Therefore, applied constant strain is calculated using below [40]:

$$\varepsilon = \frac{N_s \times dt \times V}{L} \quad (8)$$

where  $\varepsilon$  is the strain,  $N_s$  is the number of steps,  $L$  is the length of CNT and  $V$  denotes the velocity.

Prior to obtaining Young's modulus, a proper length for CNTs is chosen prohibiting unwelcomed edge effect. Unwelcomed edge effects are identified in obtained results when the CNT length is less than 5 nm. This is attributed to the restrictive boundary conditions which prohibits free vibrations of atoms. For instance, the results obtained for Young's modulus of (9, 9) CNT with respect to the length are presented in Fig. 1. The same as reported trend by Mielke et al. [13], when the CNT length increases the failure strain decreases, accordingly.

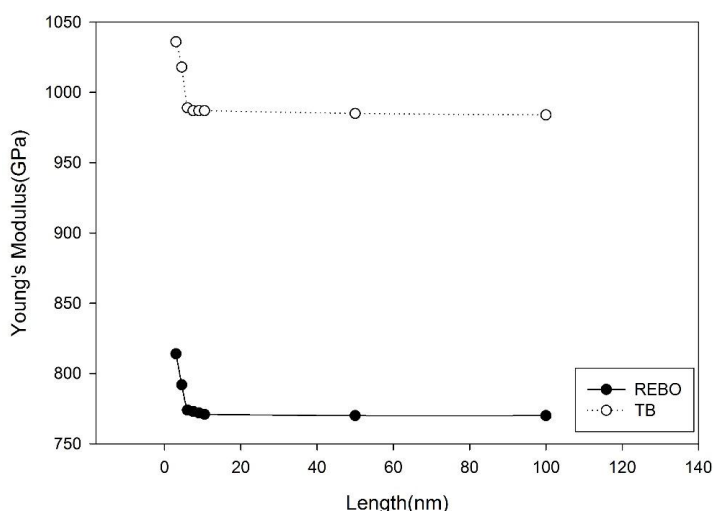


Fig. 1 Variation of CNTs Young's modulus with its length [46]

It is evident from Fig. 1 that the Young's modulus of (9, 9) CNT converges to 770 GPa for REBO potentials and 984 GPa for TB potentials for CNT lengths larger than 15 nm implying on the aspect ratio higher than 10. In other words, choosing an aspect ratio greater than 10 the edge effect diminishes. Subsequently, in all cases the length of CNTs is selected in a manner to address the aspect ratio of 10.

The stress-strain curves for a CNT with chiral index of (16, 16) as the output of simulation employing both TB and REBO potentials are presented in Fig. 2. As it was earlier mentioned, the length of CNT is selected sufficiently large to represent an aspect ratio higher than 10. Subsequently, the numerical errors on the results arisen from edge effects are avoided.

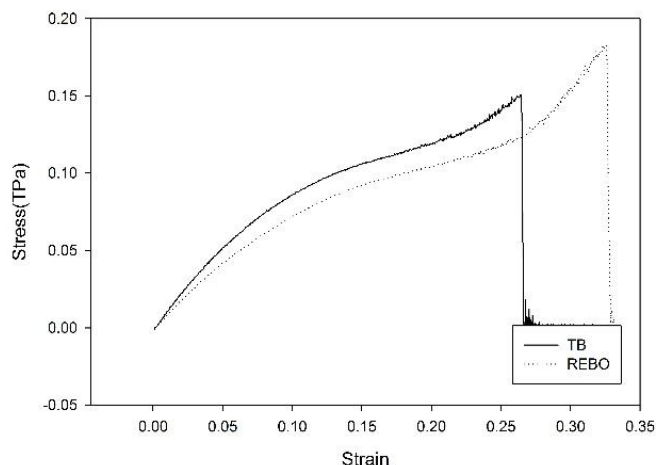


Fig. 2 Stress-strain curves for (16, 16) CNT [46]

The failure in CNT is realized by the sudden drop in stress-strain curves presented in Fig. 2 which takes place when the length of C-C bonds exceeds 2 Å for REBO case and 1.95 Å for TB case [46].

As it can be seen from Fig. 1, when REBO potential is employed, lower moduli for CNTs are captured employing in comparison with what reported by TB. This discrepancy stems from this fact that associated parameters with dihedral and bending interactions in REBO potential have considerable influence on the total potential energy.

The influence of CNT diameters and chiral indices on the Young's modulus is depicted in Fig. 3. The increasing trend of Young's modulus for both types is observed. The obtained Young's modulus of simulated CNTs is calculated in the range of 2% to 5% of strain where the linear trend in stress-strain curves can be seen.

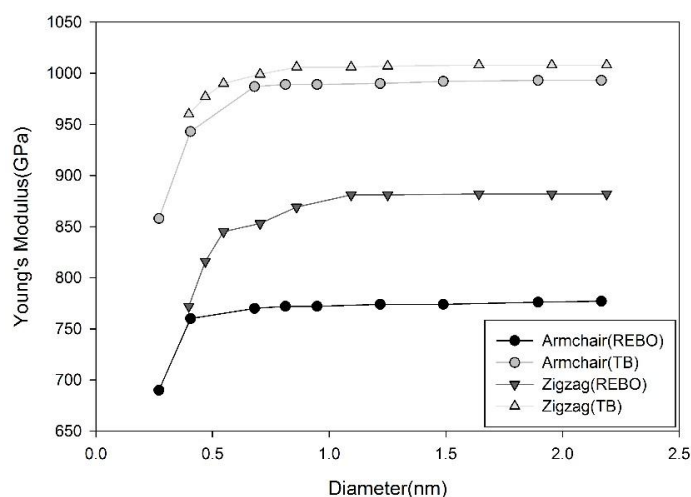


Fig. 3 Variation of CNTs Young's modulus with its diameter [46]

It is evident from the results that Young's modulus of Zigzag CNTs is higher than that of Armchair ones.

### C. Modeling Defected CNT

The influence of vacancy defect is studied in this section which is a common defect type when chemical functionalization is applied to CNT. The orbitals of carbon atom are required to be decreased from  $sp^3$  to  $sp^2$  in order to establish a strong covalent bond with surrounding polymer during functionalization procedure. As a result, transverse covalent bonds are established between CNT and surrounding polymer chains for better stress transferring from polymer to CNT. Nevertheless, this process has an important negative aspect in causing defects into CNT nano-structure. Therefore, it is essential to analyze the degree to which vacancy defects can affect the Young's modulus of CNT and consequent reduction.

Assuming numbers and locations of defects along length and circumferential directions as random parameters, stochastic MD simulations are properly conducted in LAMMPS. Carbon atoms are randomly selected and removed from the CNT nanostructure to induce the vacancy defects. As it is mentioned in Fig. 4, all induced vacancy defects are placed sufficiently far from both ends avoiding unwelcomed edge effects on the results.

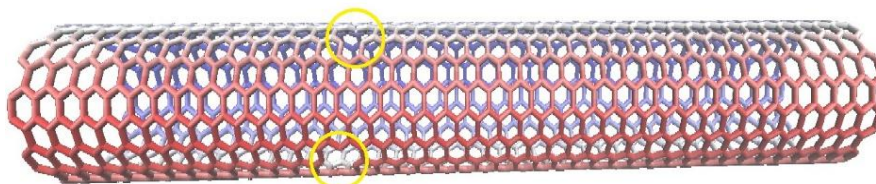


Fig. 4 Defected armchair CNT

For each specific number of defects, the modeling is repeated sufficiently to obtain a standard deviation (SD) of Young's modulus less than 1% [46]. Finally, the average of Young's modulus obtained from different realizations is reported as the Young's modulus of the investigated defected CNT.

A linear trend of reduction in Young's modulus is observed versus increasing number of defects as illustrated in Fig. 5. Moreover, the decrease rate for the Young's modulus of Zigzag CNT is more tangible than that of Armchair ones. This trend has been also reported by nano-scale continuum modeling [47].

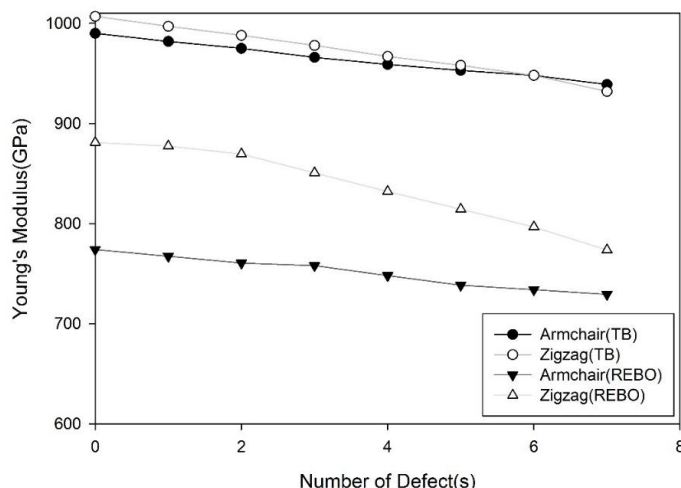


Fig. 5 Variation of defected CNTs Young's modulus with number of defects [46]

Calculated Young's modulus of defected CNTs in this study and available published data on defected CNT are compared in Table 2.

It is worth mentioning that deterministic simulations are conducted in the all mentioned studies in Table 2 except the research conducted by Rafiee and Pourazizi [47] and also the present study. Therefore, reported reductions of modulus in aforementioned investigations are presented as the ranges of reduction instead of a certain values [46].

It can be concluded that for both TB and REBO force fields, almost the same reduction is attained in the Young's modulus of defected CNTs and particularly the same reduction is achieved for the specific case of defected CNT containing one vacancy defect. On the other hand, an underestimated reduction is reported by the nano-scale continuum modelling which is broadly used by researchers as the alternative approach to atomistic modelling techniques.

It is demonstrated that the Young's moduli of CNTs are strongly sensitive to the number of vacancy defects. More importantly, defected CNTs containing more than two vacancy defects the reduction level for Young's modulus significantly depends on the locations of vacancy defects.

TABLE 2 YOUNG'S MODULUS OF DEFECTED CNT [46]

Researcher(s)	Method	Chiral Index	Number of defect(s)	Reduction of modulus (%)	Reduction of modulus in this study (%)	
					TB	REBO
Saxena and Lal [27]	MD COMPASS	(10, 10)	1	0.9	0.59-0.86	
Rafiee and Pourazizi [47]	FEM	(9, 9)	1	0.27-0.67		
Sharma et al. [14]	MD COMPASS	(9, 9)	1	2.9		
			4	15.6	2.1-6.4	1.4-6.4
Chen et al. [48]	MD	(8, 8)	6	4.8	3.44-10.05	3.75-10.21
Ghavamian et al. [10]	FEM	(10, 10)	2	1.8	0.9-2.1	1.2-2.1

### III. MODELING EMBEDDED CNT IN POLYMER

After simulating isolated CNTs (both intact and defected) in the previous section, embedded CNT in a polymer is hereinafter studied. In this context, the interaction between CNT and polymer is concentrated as the crucial issue in load transferring from polymer to CNT.

Recently, Rahmat and Hubert [49] have comprehensively reviewed the interaction studies in CNT-based nanocomposites. Measuring techniques divided into experimental observations and atomistic modeling were explained and discussed. More recently, Rafiee et al. [50] have extensively reviewed modeling methods for investigating the CNT-polymer interactions on the basis of both atomistic and continuum modeling techniques. They have outlined challenges of each modeling category. Limited theoretical studies have been concentrated on the influence of functionalization on mechanical properties of CNT-based nanocomposites.

Rafiee and Pourazizi [47] used continuum modeling to study the influence of vacancy defects induced by

functionalization on mechanical properties of a representative volume element (RVE) containing functionalized CNT, interphase and surrounding polymer. They have used 3D Finite Element (FE) modeling method assuming both numbers of defects and defects locations as random parameters. Performing a stochastic analysis, they have shown that functionalization procedure will reduce the Young's modulus of the RVE at nano/micro scale [47]. Pourakbar et al. [51] have studied the effect of functionalized CNT on the properties of RVE. Constructing a 2D model, they have replaced CNT with a solid member. They modeled covalent bonds between the CNT and the resin using beam elements. They found out that by increasing the population of covalent bonds at the interphase, the stress transferring efficiency from matrix to CNT is increased and it will converge to the results achieved from the rule of mixture, even though the rule of mixture is not valid at nanoscale [51].

Frankland et al. [52] modeled an embedded single armchair CNT in polymer using MD. They have found that the Interfacial Shear Strength (ISS) increases by forming less than 1% cross-links between the CNT and the polymer [52]. Through the MD simulation, Chowdhury and Okabe [53] reported that ISS increases from 310 MPa to 1630 MPa for a functionalized (5, 5) CNT with four chemical cross links using MD simulation on the basis of Tersoff-Brenner force field.

Although, continuum-based modeling techniques are able to facilitate modeling at nanoscale as a rational compromise in modeling, the degree to which they are able to capture the actual behavior of CNT and/or interphase at nano-scale has to be carefully investigated. On the other hand, atomistic modeling is used to accurately address the real nature of interaction between CNT and polymer while they are suffering from complex formulation and huge required runtime of analysis.

In this section, both non-modified and functionalized CNTs embedded in a polymer are analyzed using MD simulations. As it was shown in previous section, functionalization will reduce the Young modulus of isolated CNT. As a subsequent, it is vital to study the effect of functionalization in the overall modulus of CNT/polymer nanocomposites due to the formation of cross links between CNT and surrounding. For the case of functionalized CNT, stochastic approach is employed taking into account the location and number of transverse covalent links as random variables. The investigated RVE should capture CNT, polymer and interaction between CNT and polymer.

Epoxy resin is selected in this study as the host matrix for CNT. The molecular structure of Epoxy with two chains is shown in Fig. 6.

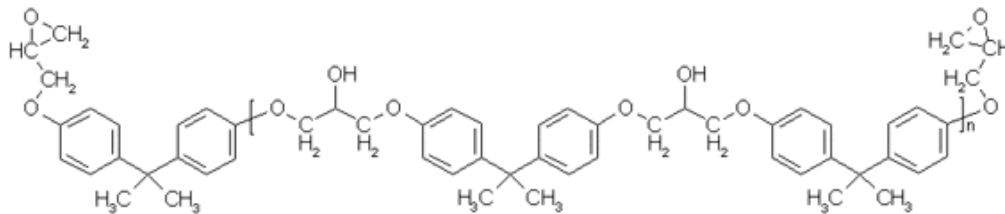


Fig. 6 Molecular structure of epoxy [54]

The covalent bond stretching in polymer chain is modeled using REBO [43] potential as explained in preceding section. Corresponding coefficients of C-C bonds are assumed as explained in Table 1, while the coefficient of C-H bonds are presented in Table 3.

TABLE 3 PARAMETERS OF THE REBO POTENTIALS FOR C-H BONDS [43]

B1 (eV)	B2 (eV)	B3 (eV)	$\alpha$ (A-1)	$\beta_1$	$\beta_2$	$\beta_3$	Q	A
32.3551	0	0	4.102	1.4344	0	0	0.340	149.9409

Due to the huge amount of atoms involved in the polymer chain, for the bond bending, linear potential is used reducing required run-time of analysis:

$$U(\theta) = \frac{1}{2} K(\theta - \theta_0)^2 \quad (9)$$

where  $K=0.9854$  Kj/mol and  $\theta_0=105.5$  for C-C bond and  $K=1.5475$  Kj/mol and  $\theta_0=109$  for C-H bonds [55].

Since the stiffness of epoxy is significantly lower than CNT, the rate of applied strain to constructed Epoxy model is 10% of the applied strain to CNT. The maximum applied strain is chosen as 2%. Fig. 7 illustrates the stress-strain curve of constructed Epoxy model where Young's modulus is obtained as 7.2 GPa.

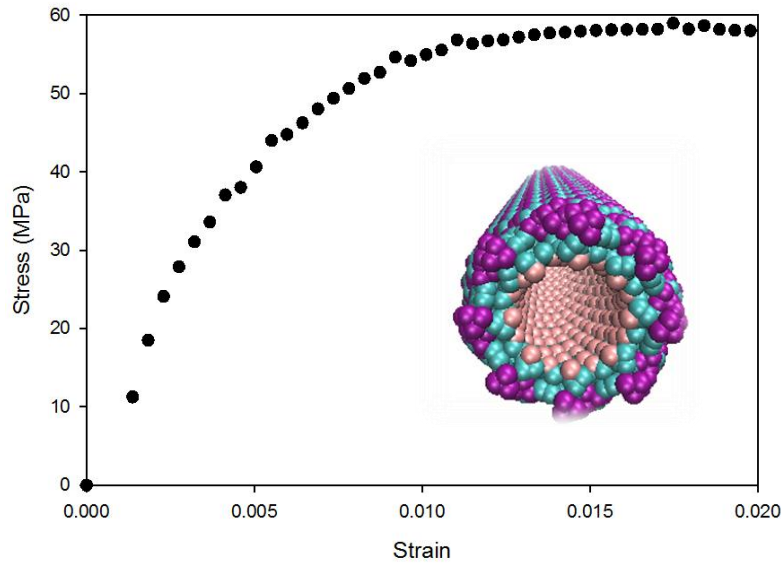


Fig. 7 Stress-strain curve for epoxy resin

A. Modeling Non-defected CNT/Polymer

The weight fraction of CNT in polymer is considered as 5%. The wrapping method is used to simulate surrounding polymer chains in investigated RVE [49]. A CNT with chiral index of (9, 9) and 15 nm length is chosen for simulation. CNT is simulated following the same procedure explained in section (2.2) on the basis of REBO potentials. The interphase is modeled using vdW non-bonded interactions. Generally, the vdW forces are derived from the Lennard–Jones “6-12” potential as below [43]:

$$F_{LJ} = 4 \frac{\epsilon}{r} \left[ -12 \left( \frac{\sigma}{r} \right)^{12} + 6 \left( \frac{\sigma}{r} \right)^6 \right] \tag{10}$$

where  $r$  is the distance between atoms. vdW parameters are also considered as  $\epsilon=0.0556$  KCal/mol and  $\sigma = 0.34$  nm. Investigated RVE is shown in Fig. 8.

The periodic boundary condition is selected and room temperature (300K) was applied in unit cell. One end of unit cell is fixed and a constant velocity is applied to the other end. The obtained result for the Young’s modulus of the RVE is 31.2 GPa.

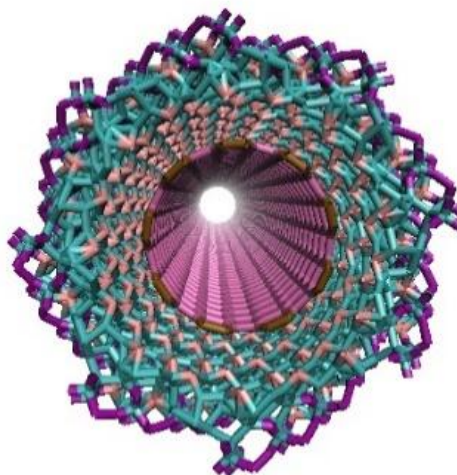


Fig. 8 Unit cell snapshot in LAMMPS software for embedded non-defected CNT in Epoxy

B. Modeling Functionalized CNT/Polymer

In this section, ten categories of embedded functionalized CNTs in polymer are simulated. One to ten C-C bonds are

removed from the CNT nanostructure representing defected CNTs. For each category, two cases of defected CNTs are modeled addressing the highest and lowest reduction in Young's modulus of isolated CNTs. These two cases are obtained as the results of performed analysis in section (2.3). In contrast to the preceding part, the interaction between CNT and polymer takes place through a combination of vdW non-bonded interactions and also transverse covalent bonds. Transverse covalent bonds are established at the same places where vacancy defects in CNT nano-structure are induced. Removing each C-C bond from CNT nanostructure, two carbon atoms can be connected transversely to surrounding polymer. Thus, each broken C-C bond will be led to the establishment of two covalent bonds between CNT and surrounding resin.

The obtained results for the Young's modulus of investigated RVE are presented in Table 4.

TABLE 4 YOUNG'S MODULUS OF RVE CONTAINING FUNCTIONALIZED CNTS [56]

Number of transverse covalent links	Reduction in CNT modulus [%]	RVE modulus [GPa]	Reduction in RVE modulus [%] (in comparison with RVE containing normal CNT)
2	0.3-0.5	31.1-31.2	0-0.3
4	1.1-1.3	31.1-31.2	0-0.3
6	1.5-1.9	31-31.2	0-0.6
8	2.0-2.9	29.9-31.1	0.3-4.2
10	2.6-4.3	29.6-31	0.6-5.1
12	3.5-5.4	29.1-31	0.6-6.7
14	5.4-6.3	28.9-29.9	4.2-7.4
16	6.2-7.4	28.6-29.4	5.8-8.3
18	7.2-9.0	28.2-29.1	6.7-9.6
20	8.5-10.7	27.8-28.8	7.7-10.9

As it can be seen from Table 4, when three C-C bonds are removed from CNT nanostructure, established six transverse covalent bonds can compensate the reduction in CNT modulus, thus the Young's modulus of the RVE does not decrease. It is revealed that the dependency of the results to the vacancy defects locations disappears when numbers of removed C-C bonds in CNT nanostructure exceeds 12 ones. In other words, beyond 12 established cross links, the Young's modulus of RVE decreases regardless of vacancy defect distribution.

It can be concluded from presented results in Table 4, generally chemical functionalization is led to a reduction in the Young's modulus of RVE at micro scale arisen from the induced considerable reduction in Young's modulus of defected CNT. This reduction is negligible for lower numbers of established cross links between CNT and polymer, while the reduction degree is amplified when the population of established cross links increases.

The influence of functionalization on the strength of the interphase region can be also investigated using the same models constructed in this section. For this purpose, CNT pull-out is simulated on the same models (embedded functionalized CNT) applying a displacement-controlled load on the carbon atoms at the right end of CNT. Furthermore, a RVE containing non-defected CNT is also analyzed for the sake of comparison.

Obtaining pull-out energy from MD simulation, the interfacial shear stress (ISS) can be computed as below [57]:

$$E_{pullout} = \int_0^L 2\pi r(L-x)\tau dx \quad (11)$$

$$\tau = \frac{E_{pullout}}{\pi L^2} \quad (12)$$

where  $r$  and  $L$  are the radius and length of CNT, respectively, and  $x$  is the displacement of the CNT. Obtained ISS for different cases are presented and compared in Table 5.

Although functionalization will be led to a reduction in the Young's modulus of the RVE in some cases because of strong influence of induced structural defects on the Young's modulus of CNT, it can increase the strength of the interphase region in all cases very significantly.

TABLE 5 THE INFLUENCE OF FUNCTIONALIZED ON ISS

Number of transverse covalent links	ISS (MPa)	Increase in ISS [%] (in comparison with RVE containing normal CNT)
0	278	0
2	1450	421.58
6	2012	623.7
8	2504	800.7
14	3230	1061.8
20	3596	1193.5

#### IV. CONCLUSIONS

The interaction between CNT and polymer is simulated using atomistic modeling. The main conclusions can be summarised by the following.

Firstly, Young's moduli of non-defected CNTs are calculated using deterministic MD simulations employing non-linear force fields. Selecting number of defects and corresponding locations at CNT nanostructure randomly, stochastic MD simulations are conducted to quantify the reduction level in CNT Young's modulus. Performing a parametric study, an increasing trend of Young's modulus versus CNT diameter is displayed, regardless of employed non-linear force fields. Moreover, Zigzag CNTs address higher values of Young's modulus in comparison with Armchair types. The difference becomes much more pronounced using REBO force fields for simulation. CNT Young's modulus becomes independent of diameter for diameters larger than one nm. CNT length study reveals that unwelcomed edge effect appears in the results for the aspect ratio (length-to-diameter) is less than 10.

Secondly, defected CNTs accommodating vacancy defects as a very common structural defect are simulated. Selecting number of defects and their corresponding locations on CNT nanostructure randomly, stochastic modeling is conducted. A linear reduction trend is observed for the Young's modulus of defected CNTs with respect to the number of vacancy defects. It was revealed that the topology of defects in CNT nano-structure can be led to a significant reduction in CNT Young's modulus (about 10%) even for those cases containing low numbers of vacancy defects.

Then, the influence of CNT functionalization on the mechanical behavior of CNT reinforced polymer was studied focusing on the interaction between CNT and surrounding polymer. After analyzing emended non-defected CNT in polymer interacting with polymer through the entirely vdW interactions, the RVE containing chemically functionalized CNT in polymer was simulated. In the later case, the interphase consists of both vdW interactions and strong covalent links between CNT and polymer. It is worth mentioning that transverse covalent links are formed in the exact locations of induced vacancy defects in CNT nano-structure. Consequently, the degree to which transverse covalent links are able to compensate the induced reduction in overall properties of the CNT reinforced polymer was analyzed. In general, it was evident from the results that chemical functionalization of the CNT reduces the Young's modulus of CNT reinforced polymer at micro scale. This is originated from the induced vacancy defects in Young's modulus of defected CNTs. It was observed that the reduction is rarely insignificant, unless low numbers of vacancy defects is induced in CNT.

It is revealed that for small populations of vacancy defects, the established cross-links between CNT and polymer can be overcome and the Young's modulus of the RVE does not decrease. But, for the higher populations of vacancy defects will be led to a considerable reduction in the Young's modulus of the RVE regardless of established cross links in the interphase region. The positive effect of chemical functionalization on the ISS of the interphase is also observed for all cases.

#### REFERENCES

- [1] B. Bhushan, *Springer Handbook of Nanotechnology*, Springer Heidelberg, 2010.
- [2] A. H. Barber, S. R. Cohen, S. Kenig, and H. D. Wagner, "Interfacial Fracture Energy Measurements for Multiwalled Carbon Nanotubes Pulled from Polymer matrix," *Composites Science & Technology*, vol. 64, pp. 2283-2289, 2004.
- [3] C. A. Cooper, D. Ravich, D. Lips, J. Mayer, and H. D. Wagner, "Load Transfer in Carbon Nanotube Epoxy Composites," *Applied Physics Letters*, vol. 81, pp. 3873-3875, 2002.
- [4] F. H. Gojny, "Carbon Nanotube Reinforced Epoxy Composites Enhanced," *Composite Science*, vol. 64, pp. 2363-2370, 2004.
- [5] A. Hernandez-Perez and F. Aviles, "Modeling the Influence of Interphase on the Elastic Properties of CNT," *Computational Materials Science*, vol. 47, pp. 926-933, 2010.
- [6] A. Neddleman, T. L. Borders, L. C. Brinson, and L. S. Shadler, "Effect of an Interphase Region on Debonding of a CNT Reinforced Polymer Composites," *Composites Science & Technology*, vol. 70, pp. 2207-2215, 2010.
- [7] R. Rafiee and R. M. Moghadam, "On the Modeling of Carbon Nanotubes: A Critical Review," *Composites Part B: Engineering*, vol. 56, pp. 435-449, 2014.

- [8] H. D. Wagner, "Nanotube Polymer Adhesion: A Mechanics Approach," *Chemical Physics Letters*, vol. 361, pp. 44-57, 2007.
- [9] P. M. Agrawal, B. S. Sudalayandi, L. M. Raff, and R. Komandari, "A comparison of different methods of Young's Modulus determination for SWCNT using MDS," *Computational Materials Science*, vol. 38, pp. 271-281, 2006.
- [10] A. Ghavamian, M. Rahmandoust, and A. Ochsner, "A numerical evaluation of the influence of defects on the elastic modulus of single and multi-walled carbon nanotubes," *Computational Materials Science*, vol. 62, pp. 110-116, 2012.
- [11] M. Chawl, "Influence of vacancy defects on the mechanical behavior and properties of carbon nanotubes," *Procedia Engineering*, vol. 10, pp. 1579-1584, 2011.
- [12] Y. R. Jeng, P. C. Tsai, and T. H. Fang, "Effects of temperature and vacancy defects on tensile deformation of single-walled carbon nanotubes," *Journal of Physics and Chemistry of Solids*, vol. 65, pp. 1849-1856, 2004.
- [13] S. L. Mielke, D. Troya, S. Zhang, J. L. Li, S. Xiao, R. Car, R. S. Ruoff, G. C. Schatz, and T. Belytschko, "The role of vacancy defects and holes in the fracture of carbon nanotubes," *Chemical Physics Letters*, vol. 390, pp. 413-420, 2004.
- [14] K. Sharma, K. K. Saxena, and M. Shukla, "Effect of Multiple Stone-Wales and Vacancy Defects on the Mechanical Behavior of Carbon Nanotubes Using Molecular Dynamics," *Procedia Engineering*, vol. 38, pp. 3373-3380, 2012.
- [15] J. Yuan and K. M. Liew, "Effects of vacancy defect reconstruction on the elastic properties of carbon nanotubes," *Carbon*, vol. 47, pp. 1526-1533, 2009.
- [16] H. C. Cheng, Y. L. Liu, Y. C. Hsu, and W. H. Chen, "Atomistic-continuum modeling for mechanical properties of single-walled carbon nanotubes," *International journal of solids and Structures*, vol. 46, pp. 1695-1704, 2009.
- [17] K. Chandrasekar and S. Mukherjee, "Atomistic-continuum and ab initio estimation of the elastic moduli of single-walled carbon nanotubes," *Computational Materials Science*, vol. 40, pp. 147-158, 2007.
- [18] K. Mylvaganam and L. C. Zhang, "Important issues in a molecular dynamics simulation for characterising the mechanical properties of carbon nanotubes," *Carbon*, vol. 42, pp. 2025-2032, 2004.
- [19] D. G. Robertson, D. W. Brenner, and J. W. Mintmire, "Energies of nanoscale graphitic tubule," *Physics*, vol. 45, pp. 12592-12595, 1992.
- [20] C. F. Cornwell and L. R. Wille, "Elastic properties of single-walled carbon nanotubes in compression," *Solid State Communication*, vol. 101, pp. 558-558, 1997.
- [21] T. Halicuglu, "Stress calculation for carbon nanotubes," *Thin solid Films*, vol. 312, pp. 11-14, 1998.
- [22] H. W. Zhang, J. B. Wang, and X. Guo, "Predicting the elastic properties of single-walled carbon nanotubes," *Mechanic Physics Solids*, vol. 53, pp. 1929-1950, 2005.
- [23] K. Talukdar and A. K. Mitra, "Comparative MD simulation study on the mechanical properties of a zigzag single-walled carbon nanotube in the presence of Stone-Thrower-Wales defects," *Composite structures*, vol. 92, pp. 1701-1705, 2010.
- [24] K. M. Liew, X. Q. He, and C. H. Wong, "On the study of elastic and plastic properties of multi-walled carbon nanotubes under axial tension using molecular dynamics simulation," *Acta Materialia*, vol. 52, pp. 2521-2527, 2004.
- [25] B. W. Xing, Z. C. Chun, and C. W. Zhao, "Simulation of Young's Modulus of single-walled carbon nanotubes by molecular dynamics," *Physica B*, vol. 352, pp. 156-163, 2004.
- [26] M. Meo and M. Rossi, "A molecular-mechanics based finite element model for strength prediction of single wall carbon nanotubes," *Materials Science and Engineering*, vol. 454, pp. 170-177, 2007.
- [27] K. K. Saxena and A. Lal, "Comparative molecular dynamics simulation study of mechanical properties of carbon nanotubes with number of stone-wales and vacancy defects," *Procedia Engineering*, vol. 38, pp. 2347-2355, 2012.
- [28] S. Sharma, R. Chandra, P. Kumar, and N. Kumar, "Effect of Stone-Wales and vacancy defects on elastic moduli of carbon nanotubes and their composites using molecular dynamics simulation," *Computational Materials Science*, vol. 86, pp. 1-8, 2014.
- [29] E. Hernandez, C. Goze, P. Bernier, and A. Rubio, "Elastic properties of single-wall nanotubes," *Applied Physics*, vol. 68, pp. 287-292, 1999.
- [30] D. S. Portal, E. Artacho, J. M. Soler, A. Rubio, and P. Ordejon, "Ab initio structural, elastic, and vibrational properties of carbon nanotubes," *Physics Review*, vol. 59, pp. 12678-12688, 1999.
- [31] J. M. Molina, S. S. Savinsky, and N. V. Khokhriakov, "A tight-binding model for calculations of structures and properties of graphitic nanotubes," *Journal of Chemical Physics*, vol. 104, pp. 4652-4656, 1996.
- [32] C. Goze, L. Vaccarini, L. Henard, P. Bernier, E. Hernandez, and A. Rubio, "Elastic and mechanical properties of carbon nanotubes," *Synthetic Metal*, vol. 103, pp. 2500-2501, 1999.
- [33] L. Vaccarini, C. Goze, L. Henard, E. Hernandez, P. Bernier, and A. Rubio, "Mechanical and electronic properties of carbon and boron-nitride nanotubes," *Carbon*, vol. 38, pp. 1681-1690, 2000.
- [34] Z. Xin, Z. Jianjun, and O. Y. Z. Can, "Strain energy and Young's Modulus of single-wall carbon nanotubes calculated from electronic energy-band theory," *Physics Review*, vol. 62, pp. 13692-13696, 2000.
- [35] G. V. Lier, C. V. Alsenoy, V. V. Doren, and P. Geerlings, "Ab initio study of the elastic properties of single-walled carbon nanotubes and grapheme," *Chemical Physics Letter*, vol. 326, pp. 181-185, 2000.
- [36] K. N. Kudin, G. E. Scuseria, and B. I. Yakobson, "F, BN, and C nanoshell elasticity from ab initio computations," *Physics Review*, vol. 64, pp. 235-306, 2001.
- [37] J. Cai, Y. D. Wang, and C. Y. Wang, "Effect of ending surface on energy and Young's Modulus of singlewalled carbon nanotubes studied using linear scaling quantum mechanical method," *Physica B*, vol. 404, pp. 3930-3934, 2009.
- [38] M. M. Shokrieh and R. Rafiee, "A Review of the Mechanical Properties of Isolated Carbon Nanotube Composites," *Mechanics of Composites Materials*, vol. 46, pp. 155-172, 2010.
- [39] E. G. Fefey, R. Mohan, and A. Kelkar, "Computational study of the effect of carbon vacancy defects on the Young's Modulus of (6, 6)

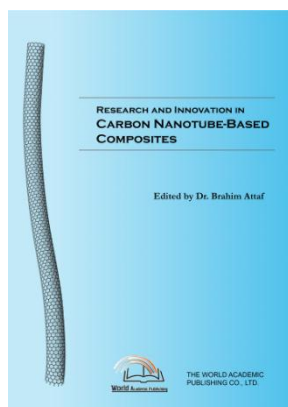
- single wall carbon nanotube,” *Materials Science and Engineering*, vol. 176, pp. 693-700, 2011.
- [40] H. Rafiee-Tabar, *Computational Physics of Carbon Nanotubes*, New York: Cambridge University Press, 2008.
- [41] W. D. Cornell, P. Cieplak, and C. I. Bayly, “A Second Generation Force Field for the Simulation of Proteins, Nucleic Acids, and Organic Molecules,” *American Chemical Society*, vol. 117, pp. 5179-5197, 1995.
- [42] J. Tersoff, “Empirical Interatomic Potential for Carbon, with Applications to Amorphous Carbon,” *PHYSICAL REVIEW LETTERS*, vol. 61, pp. 2879-2882, 1988.
- [43] D. W. Brenner, O. A. Shenderova, J. A. Harrison, S. J. Stuart, B. Ni, and S. B. Sinnott, “A second-generation reactive empirical bond order (REBO) potential energy expression for hydrocarbons,” *JOURNAL OF PHYSICS: CONDENSED MATTER*, vol. 14, pp. 783-802, 2002.
- [44] T. Belytschk, S. Xiao, G. Schatz, and R. Ruoff, “Atomistic Simulations of Nanotube Fracture,” *Physical Review B*, vol. 65, pp. 235-262, 2002.
- [45] LAMMPS User’s Manual, Sandia Corporation. Jan 2013 Version.
- [46] R. Rafiee and M. Mahdavi, “Molecular dynamics simulation of defected carbon nanotubes,” *Proceedings of the Institution of Mechanical Engineers Part L Journal of Materials Design and Applications*, DOI: 10.1177/1464420715584809.
- [47] R. Rafiee and R. Pourazizi, “Evaluating the influence of defects on the Young’s Modulus of carbon nanotubes using stochastic modelling,” *Material Research*, vol. 17, pp. 758-766, 2014.
- [48] L. Chen, Q. Zhao, Z. Gong, and H. Zhang, “The effects of different defects on the elastic constants of single-walled carbon nanotubes,” In: *Proceedings of the 5th IEEE International Conference on Nano/Micro Engineered and Molecular Systems*, Xiamen, China, 2010.
- [49] M. Rahmat and P. Hubret, “Carbon nanotube–polymer interactions in nanocomposites: A review,” *Composites Science & Technology*, vol. 72, pp. 72-84, 2011.
- [50] R. Rafiee, T. Rabczuk, R. Pourazizi, J. Zhao, and Y. Zhang, “Challenges of the Modeling Methods for Investigating the Interaction between the CNT and the Surrounding Polymer,” *Advances in Materials Science and Engineering*, vol. 2013, pp. 1-10, 2013.
- [51] K. Pourakbar, N. JamilPour, A. R. Najafi, G. Rouhi, A. Arshi, and A. Fereidoon, “A finite element model for estimating Young’s modulus of carbon nanotube reinforced composites incorporating elastic cross-links,” *Engineering and Technology*, vol. 2, pp. 181-184, 2008.
- [52] S. J. V. Frankland, A. Caglar, D. W. Brenner, and M. Griebel, “Molecular Simulation of the Influence of Chemical Cross-Links on the Shear Strength of Carbon Nanotube-Polymer Interfaces,” *Journal of Physical Chemistry*, vol. 106, pp. 3046-3048, 2002.
- [53] S. C. Chowdhury and T. Okabe, “Computer Simulation of Carbon Nanotube Pull-Out from Polymer,” *Composites: Part B*, vol. 38, pp. 747-754, 2007.
- [54] V. Lordi and N. Yao, “Molecular mechanics of binding in carbon-nanotube–polymer composites,” *Journal of Materials Research*, vol. 15, pp. 2770-2779, 2000.
- [55] S. J. Plimpton, “Fast Parallel Algorithms for Short-Range Molecular Dynamics. Journal of Computational Physics,” *Journal of Computational Physics*, vol. 117, pp. 1-19, 1995.
- [56] R. Rafiee and M. Mahdavi, “Characterizing nanotubes-polymer interaction using molecular dynamics simulation,” *Computational Materials Science*, DOI: 10.1016/j.commatsci.2015.10.041.
- [57] Y. Li, Y. Liu, X. Peng, and N. Hu, “Pull-Out Simulations on Interfacial Properties of Carbon Nanotube-Reinforced,” *Computational Materials Science*, vol. 50, pp. 1854-1860, 2011.



**Dr. Roham RAFIEE** has received his PhD in 2010 in mechanical engineering Dept. of Iran University of Science and Technology focusing on nanocomposites. He has done his MSc and BSc theses in the field of composite materials and structures.

Roham has 15 years of experience in different industrial sections including wind turbines, composite pipes, strategic planning and technology transfer projects. His research interests can be summarized as carbon nanotube reinforced polymers, mechanics of composite materials, design and analysis of composite structures, fatigue modelling of composite structures, finite element modelling and analysis. He is currently an associate professor of the Faculty of New Sciences and Technologies in University of Tehran. He is already the vice president of Iranian Composites Association. He is also senior consultant of different companies and industrial group. He is currently cooperating with University of Weimar (Germany) as a member of PhD community and also UPM (Malaysia) as an advisor of PhD thesis. He is the founder and director of Composites Research Laboratory ([www.COMRESLAB.com](http://www.COMRESLAB.com)) in university of Tehran.

Dr. Rafiee, has published 35 ISI papers, 47 international conference papers and five book chapters in Woodhead publishing, Springer, Taylor & Francis and World academic publishing. He has also registered three patents in the field of nanocomposites and composite structures. He was selected as distinguished researcher in Faculty of New Sciences and Technologies on 2014.

**Research and Innovation in Carbon Nanotube-Based Composites**

Edited by Dr. Brahim Attaf

ISBN 978-0-9889190-1-3

Hard cover, 136 pages

**Publisher:** The World Academic Publishing Co. Ltd.**Published in printed edition:** 30, December 2015**Published online:** 30, December 2015

This book of nanoscience and nanotechnology provides an overview for researchers, academicians and industrials to learn about scientific and technical advances that will shape the future evolution of composite materials reinforced with carbon nanotubes (CNTs). It involves innovation, addresses new solutions and deals with the integration of CNTs in a variety of high performance applications ranging from engineering and chemistry to medicine and biology. The presented chapters will offer readers an open access to global studies of research and innovation, technology transfer and dissemination of results and will respond effectively to challenges related to this complex and constantly growing subject area.

**How to cite this book chapter**

Roham Rafiee and Mohammad Mahdavi (2015). On the Interfacial Properties of Carbon Nanotube Based Composites, *Research and Innovation in Carbon Nanotube-Based Composites*, Dr. Brahim Attaf (Ed.), ISBN 978-0-9889190-1-3, WAP-AMSA, Available from: <http://www.academicpub.org/amsa/>

**World Academic Publishing - Advances in Materials Science and Applications**